

Largest connected component in duplication-divergence growing graphs with symmetric coupled divergence

Dario Borrelli^{1,*}

¹ *Theoretical Physics Div., University of Naples Federico II, I-80125, Naples, Italy*

(Dated: January 27, 2026)

The largest connected component in duplication-divergence growing graphs with symmetric coupled divergence is studied. Finite-size scaling reveals a phase transition occurring at a divergence rate δ_c . The δ_c found stands near the locus of zero in Euler characteristic for finite-size graphs, known to be indicative of the largest connected component transition. The role of non-interacting vertices in shaping this transition with their presence ($d = 0$) and absence ($d = 1$) in duplication is also discussed, suggesting a particular transformation of the time variable considered, which yields a singularity locus in the natural logarithm of the absolute value of Euler characteristic in finite-size graphs near to that obtained with $d = 1$ but from the model with $d = 0$. The findings may suggest implications for bond percolation in these growing graph models.

Duplication-divergence graph models are a type of sequentially growing network models [1–7] aimed at the understanding of structural characteristics of different kinds of complex systems represented through the abstraction of graphs [8–19] (for a review see Ref. [20] and references therein). Duplication refers to exact copy of an existing vertex of the network, namely the original vertex i , into a copy vertex i' having the same edges; divergence refers to probabilistic loss or conservation of duplicate edges. The divergence process in such a network growth model considers the divergence probability $\delta \in [0, 1]$, also known as divergence rate, while the extent to which edges are conserved or lost from i or from i' considers the so-called divergence asymmetry rate $\sigma \in [0, 1]$, from Ref. [19].

In a coupled divergence process, for each duplicate edge pair resulting from duplication, i.e., $i \bullet \dots \bullet i'$, one can write the probabilities of transitioning to the configuration indicated in parentheses on the left hand side of the following equations

$$\begin{aligned} \mathcal{P}(i \bullet \dots \bullet i') &= 1 - \delta, \\ \mathcal{P}(i \bullet \dots \bullet i') &= (1 - \sigma)\delta, \\ \mathcal{P}(i \bullet \dots \bullet i') &= \sigma\delta. \end{aligned} \quad (1)$$

In coupled symmetric divergence, $\sigma = 1/2$ is assumed in Eqs. (1), thus, a pair of duplicate edges can lose one of the two edges linked to the same adjacent vertex from either the original or the copy vertex, with equal probability. In a general duplication-divergence model with non-complete asymmetric divergence ($\sigma \neq 0, 1$), prior work showed the emergence of connected components of heterogeneous size $s > 1$ [19], which also holds for the symmetric coupled case here considered, with $\sigma = 1/2$. This observation motivates a deeper understanding of structural changes in graphs resulting from the duplication-divergence model with symmetric coupled divergence, with the focus here on the largest connected component of this sequentially growing network model.

In duplication, an existing vertex to be duplicated is randomly chosen among existing vertices, with $d = 1$ when duplication reflects a random uniform choice among the set of vertices with at least one edge (interacting vertices), and with $d = 0$ when it reflects a random uniform choice among all vertices, including those with no edges (non-interacting vertices) [19].

Given an initial graph with only two connected vertices, and being t the total number of vertices of the growing graph but also a discrete time variable counting the number of iterations ($\Delta t = 1$) as in Ref. [19], with $d = 1$, and from (1), the expected number of interacting vertices $N(\delta, t)$ increases according to

$$\frac{\Delta N(\delta, t)}{\Delta t} = \sum_{k=1}^{\infty} n_k [1 - (\sigma\delta)^k - (\delta - \sigma\delta)^k], \quad (2)$$

where n_k is the expected fraction of k -degree vertices. In symmetric coupled divergence ($\sigma = 1/2$), and with $\delta \geq 1/2$, expliciting the series one gets

$$\frac{\Delta N(\delta, t)}{\Delta t} \propto \left[(1 - \delta) + \left(1 - \frac{\delta^2}{2}\right) 2^{-\gamma} + \dots \right], \quad (3)$$

with the assumption of $n_k \sim k^{-\gamma}$ from Ref. [19]. It turns out that stopping at the first term of the series provides a good approximation for what hereafter discussed, while in general may be not. For this purpose, according to Ref. [19], the proportionality in (3) is substituted with a prefactor of 2, yielding to consider in the large k limit, the following form (see Appendix A)

$$N(\delta, t) \simeq 2(1 - \delta)t. \quad (4)$$

The expected number of edges $E(\delta, t)$, with an initial graph with two connected vertices, has been provided in Ref. [19], being (see Appendix B)

$$E(\delta, t) = \frac{\Gamma(2 - 2\delta + t)}{\Gamma(t)\Gamma(4 - 2\delta)}, \quad (5)$$

with $\Gamma(\cdot)$ the Euler Gamma function. Note that, for increasingly large t , the model with $d = 0$ shows the growth

* dario.borrelli@unina.it

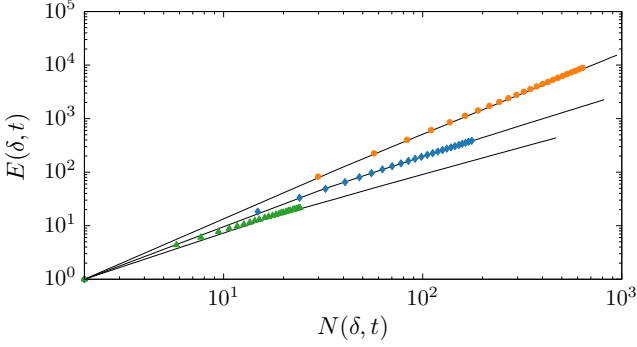


FIG. 1. Growth of $E(\delta, t)$ versus $N(\delta, t)$ with symmetric coupled divergence ($\sigma = 1/2$), for $d = 0$ (points) and $d = 1$ (solid curves), for various δ : 0.25 (\circ), 0.5 (\diamond), 0.75 (\triangle). Points and curves shown result from averaging over 10^2 simulations ending with a total number of vertices $t = 10^3$.

pattern of $E(\delta, t)$ versus $N(\delta, t)$ of the model with $d = 1$, see Fig. 1, yet described by Eq. (5) with t (as shown in Ref. [19]).

The relevant difference between the model with $d = 0$ and the model with $d = 1$ stands in the mean number of edges given a fixed t , due to the non-uniform probability distribution of choosing a vertex for duplication, which is non-zero only for k -degree vertices with $k \geq 1$ when $d = 1$. In Ref. [21], it has been shown that topological transitions can be found through the Euler characteristic of a simplicial complex, and for the special case of a duplication-divergence graph with complete asymmetric divergence ($\sigma = 1$). The Euler characteristic is defined as $\sum_n (-1)^n \kappa_n$, where κ_n is the total number of n -cliques. Then, as in Ref. [21], for the special case of a duplication-divergence graph, which does not include n -cliques with $n \geq 3$, the Euler characteristic assumes the form $t - E(\delta, t)$ (with t the total number of vertices in the graph), and the Euler entropy is the natural logarithm of its absolute value, $\ln|t - E(\delta, t)|$. Thus, zeros of the Euler characteristic correspond to singularities in the Euler entropy [21]. A locus of singularity in Euler entropy – here denoted by $\delta_{c,\xi}$ – arises at the formation of n -cycles [21]. Since δ affects the probability of losing edges due to the divergence process, then $\delta_{c,\xi}$ should be slightly higher than a critical value δ_c , where the largest connected component transition occurs. Fig. 2 shows for finite-sized graphs a $\delta_{c,\xi} \approx 0.442$ (see Appendix B) that agrees with the result for complete asymmetric divergence ($\sigma = 1$) in Ref. [21] although here, instead, it is found for the symmetric coupled divergence case ($\sigma = 1/2$) of the model with $d = 0$. The Euler entropy of finite-sized graphs for the model with $d = 1$ has been estimated numerically, leading to $\delta_{c,\xi} \approx 1 - e^{-1}$ (see, Fig. 2(d)).

Due to a different number of non-interacting vertices, (4) may not directly hold for the model with $d = 0$, nonetheless, the mean number of edges of interacting vertices can be matched across the case of $d = 0$ and $d = 1$ (Fig. 1), and one can get the corresponding t (as

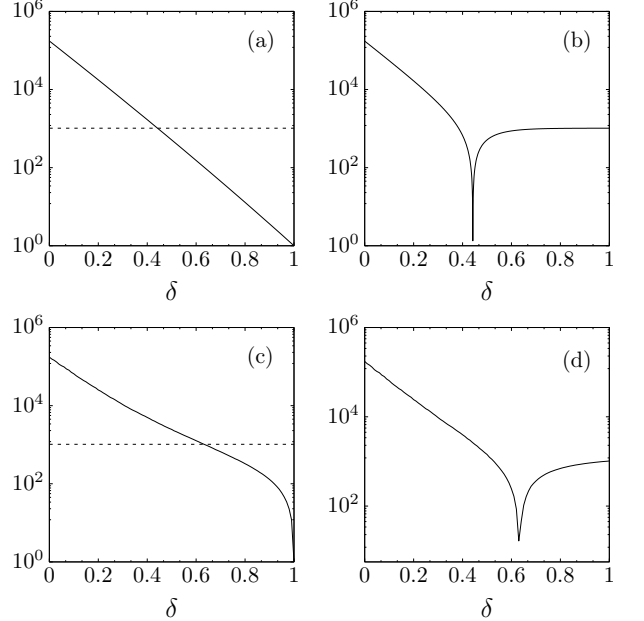


FIG. 2. Plots of $E(\delta, t)$ and t with $t = 1024$, respectively with solid and dashed lines in left panels: in (a) with $d = 0$, and in (c) with $d = 1$. In (b), $|t - E(\delta, t)|$ (solid curve on right panels) for the model with $d = 0$ showing a locus of singularity at $\delta_{c,\xi} \approx 0.442$, while in (d) Euler entropy with $d = 1$, with $\delta_{c,\xi} \approx 1 - e^{-1}$. Solid curves in (a),(b) are obtained through Eq. 5, while in (c),(d) through averaging over 10^3 simulations.

if the model was with $d = 1$) from the model with $d = 0$, through the transformation (with $\delta \neq 1$)

$$t'(\delta, t) \simeq N(\delta, t)/2(1 - \delta). \quad (6)$$

Note that t' is a δ -dependent function and not a fixed value as in the calculation of the Euler entropy shown in Fig. 2. It is suggested that $t'(\delta, t)$ has also a scaling form for increasing t in a subset of δ values where curves for various t collapse on the same function. The ansatz considered here for this scaling of $t'(\delta, t)$ is

$$t'(\delta, t) = t^{-w/\varphi} h \left[(\delta - \delta_c) t^{1/\varphi} \right], \quad (7)$$

with w , φ , $h(\cdot)$ respectively two unknown exponents and a scaling function. Different curves for various t collapse on the same curve for $\delta \in [0.55, 0.75]$ (see Fig. 3), with $\delta_c = 0.638 \pm 0.006$, $w = 2.831 \pm 0.095$, $\varphi = 4.177 \pm 0.367$, which is indeed the range of δ -values where $\delta_{c,\xi}$ is expected in the model with $d = 1$. Intriguingly, the transformation $t'(\delta, t)$ on the model with $d = 0$ can be leveraged to get an Euler entropy curve different from the one estimated numerically for the model with $d = 1$, yet exhibiting nearly the same singularity locus of the Euler entropy for finite-sized graphs, that is $\delta_{c,\xi} \approx 1 - e^{-1}$, as it is shown in Fig. 4.

Now, the ansatz for the probability of a vertex to belong to the largest connected component $P(\delta, t)$ is written

$$P(\delta, t) = t^{\zeta/\nu} f \left[(\delta - \delta_c) t^{1/\nu} \right], \quad (8)$$

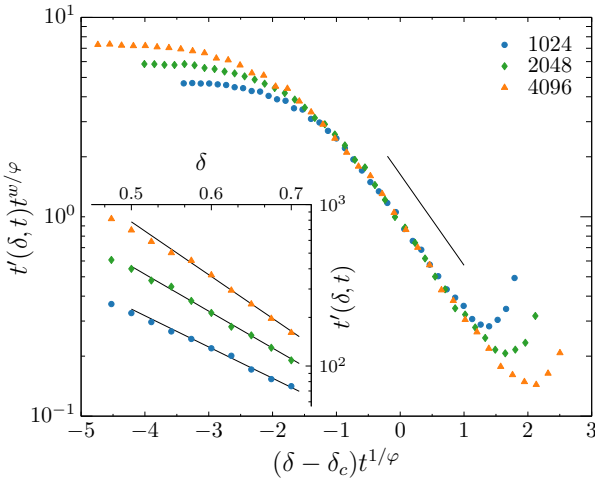


FIG. 3. Finite-size scaling for $t'(\delta, t)$ showing scaling collapse for $\delta \in [0.55, 0.75]$. The linear behavior in log-linear plot suggests the exponential form (shown for visual reference), $ae^{-b(\delta-\delta_c)t^{1/\varphi}}$ with $a \approx 0.95$, $b \approx 1.05$ which, when unscaled, describes a subset of points of $t'(\delta, t)$ versus δ (see inset).

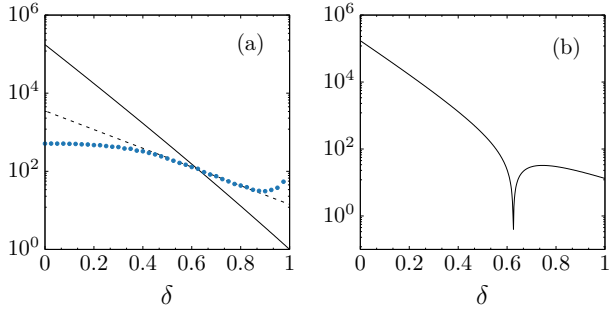


FIG. 4. In (a), $E(\delta, t)$ (solid line), $t'(\delta, t)$ (dashed line) as in inset of Fig. 3, simulations (points with \circ). In (b), Euler entropy curve assuming $t'(\delta, 1024)$ in the model with $d = 0$, with $\delta \in [0.55, 0.75]$ from Fig. 3 extended for visual reference to $\delta \in [0, 1]$. The singularity has a locus near $\delta_{c,\xi} \approx 1 - e^{-1}$ as the one for $d = 1$ in Fig. 2(d).

where ζ , ν , $f(\cdot)$ are respectively two unknown exponents and a scaling function on which one would expect scaling collapse of $P(\delta, t)$ for various sizes t , i.e., various graph order in the language of graph theory. Denoting $P_\infty := P(\delta, t)$, and the susceptibility of P_∞ with

$$\chi(\delta, t) = t \left(\langle P_\infty^2 \rangle - \langle P_\infty \rangle^2 \right), \quad (9)$$

which characterizes the intensity of fluctuation about the mean order parameter, then the following scaling ansatz for the susceptibility is also written

$$\chi(\delta, t) = t^{\psi/\nu} g \left[(\delta - \delta_c)t^{1/\nu} \right], \quad (10)$$

with ψ an unknown exponent, and $g(\cdot)$ a scaling function. For the largest connected component, the value δ_c here found slightly precedes the locus $\delta_{c,\xi}$ as anticipated. Indeed, it turns out that the collapse on the same curve

is obtained for $\delta_c = 0.6 \pm 0.002$, $\zeta = -0.033 \pm 0.059$ and $\nu = 9.634 \pm 0.069$ (see Fig. 5), and ψ determined by satisfying the following relation (scaling is in terms of “volume”, total number of vertices t)

$$\psi/\nu = 1 + 2\zeta/\nu. \quad (11)$$

Note that, from Eqs. (1), $p = 1 - \delta$ would link what here studied to a bond percolation on growing graphs while the exponents may be reminiscent of those of an explosive transition with trivial exponents $\zeta = 0$ and $\psi/\nu = 1$ according to relations between exponents in [22, 23], with some plausible analogy to jamming [24]; yet, the estimated exponent ζ is non-zero and of the order of 10^{-2} (extremely small), thus only $\zeta \approx 0$ and $\psi/\nu \approx 1$, which also suggests to consider this transition as continuous [25, 26]. At the critical value δ_c , in Fig. 6, the exponent ψ/ν describes the scaling of peaks χ^* of $\chi(\delta, t)$, for various t , and $\langle s \rangle^*$ of the weighted average connected component size $\langle s \rangle$, the latter defined as (with $\sum_s s C_s(\delta, t) \neq s_\infty$)

$$\langle s \rangle = \frac{\sum_s s^2 C_s(\delta, t) - s_\infty^2}{\sum_s s C_s(\delta, t) - s_\infty}, \quad (12)$$

with $C_s(\delta, t)$ and s_∞ respectively the expected number of connected components of size s and size of the largest connected component. Indeed, at the critical point, one would expect (see also Appendix C)

$$\chi(\delta_c, t) \sim t^{\psi/\nu}, \quad (13)$$

provided that the estimates of ψ and ν are correct [27].

As previously discussed for the calculation of Euler entropy, the role of non-interacting vertices appears to be crucial in changing the locus of the critical value in topological transitions of the duplication-divergence graph model with symmetric coupled divergence. From such

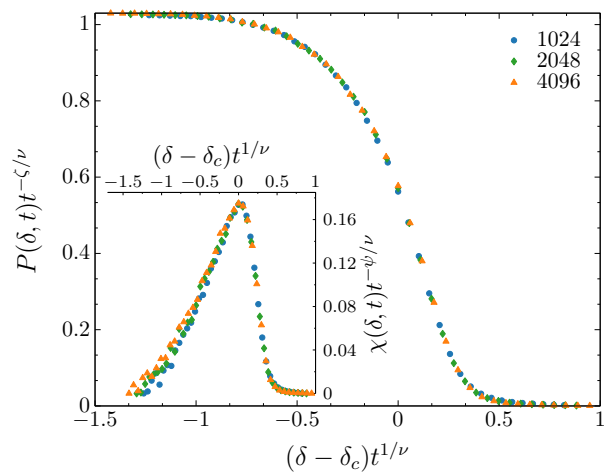


FIG. 5. Scaling collapse of $P(\delta, t)$ and $\chi(\delta, t)$ (inset), respectively from Eq. 8 and Eq. 10. Each point is obtained by averaging over $3 \cdot 10^3$ simulations ending at a different total number of vertices t (in legend).

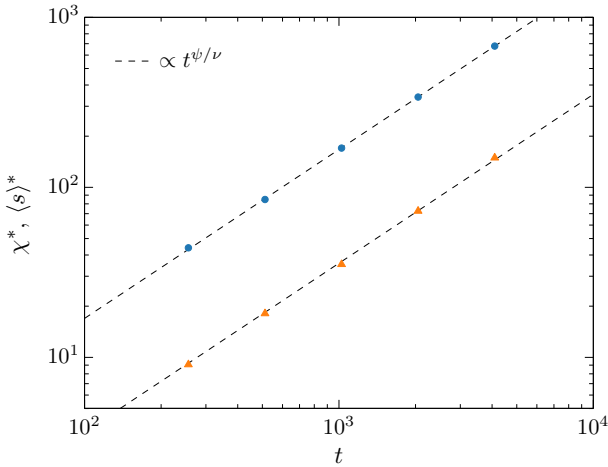


FIG. 6. Scaling with t of χ^* (points with \circ) and $\langle s \rangle^*$ (points with \triangle) for increasing sizes t : 256, 512, 1024, 2048, 4096. Dashed lines are visual references for the scaling $t^{\psi/\nu}$.

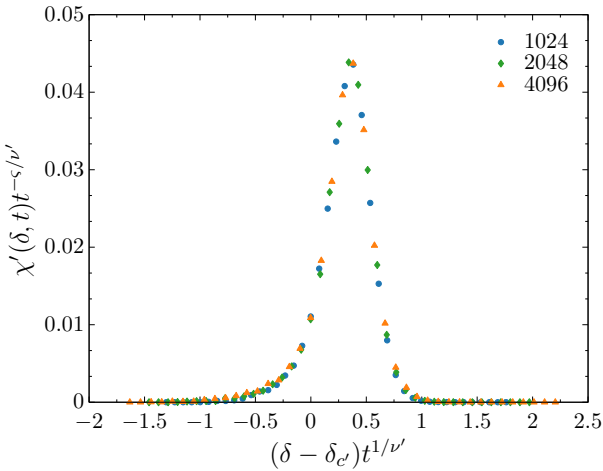


FIG. 7. Scaling collapse of $\chi'(\delta, t)$, with $\delta_{c'} = 0.425 \pm 0.001$ which preceedes $\delta_{c,\xi}$ shown in Fig. 2(b) for $d = 0$; $\chi'(\delta, t)$ quantifies the fluctuation about $\langle s' \rangle$.

a consideration, therefore, one can further define the following observable $\langle s' \rangle = \sum_{s>1} s C_s(\delta, t) / \sum_{s>1} C_s(\delta, t)$, being it an unconventional average connected component size in which non-interacting vertices ($s = 1$) have not been considered in the sum. Then, one can consider

$$\chi'(\delta, t) = (\langle s'^2 \rangle - \langle s' \rangle^2) / N(\delta, t) \quad (14)$$

proportional to the fluctuation about the mean quantity $\langle s' \rangle$. Then for χ' , a different scaling ansatz is written

$$\chi'(\delta, t) = t^{\varsigma/\nu'} \ell \left[(\delta - \delta_{c'}) t^{1/\nu'} \right], \quad (15)$$

with ς, ν' two unknown exponents and $\ell(\cdot)$ a scaling function on which one may expects collapse of curves for various t with the correct choice of the exponents and of $\delta_{c'}$. The estimated exponent is $\nu' = 6.185 \pm 0.002$, with the

scaling collapse occurring for $\varsigma = 6.827 \pm 0.002$, see Fig. 7. The value of $\delta_{c'} = 0.425 \pm 0.001$, slightly anticipates the value $\delta_{c,\xi} \approx 0.442$ found for the model with $d = 0$. While in the model with $d = 1$ at the critical point δ_c there may be a scaling $\langle s \rangle \propto t^{\psi/\nu}$ (see Fig. 6), I also observed that, slightly away from δ_c the scaling similarly holds, e.g., at $\delta = 1/2$. Noteworthy is that the estimated $\delta_{c'}$ preceeds $1/2$ which it may occur presumably with, e.g., slow dimerization, mutation rates [18], yet it is also worth noting that non-interacting vertices have a relevant role in shaping the transition studied.

- [1] P. L. Krapivsky, S. Redner, and F. Leyvraz, *Phys. Rev. Lett.* **85**, 4629 (2000).
- [2] S. N. Dorogovtsev, J. F. F. Mendes, and A. N. Samukhin, *Phys. Rev. Lett.* **85**, 4633 (2000).
- [3] R. Albert and A.-L. Barabási, *Phys. Rev. Lett.* **85**, 5234 (2000).
- [4] P. L. Krapivsky and S. Redner, *Phys. Rev. E* **63**, 066123 (2001).
- [5] E. M. Jin, M. Girvan, and M. E. Newman, *Phys. Rev. E* **64**, 046132 (2001).
- [6] D. S. Callaway, J. E. Hopcroft, J. M. Kleinberg, M. E. Newman, and S. H. Strogatz, *Phys. Rev. E* **64**, 041902 (2001).
- [7] A. Vázquez, *Phys. Rev. E* **67**, 056104 (2003).
- [8] R. V. Solé, R. Pastor-Satorras, E. Smith, and T. B. Kepler, *Adv. Complex Syst.* **5**, 43 (2002).
- [9] J. Kim, P. Krapivsky, B. Kahng, and S. Redner, *Phys. Rev. E* **66**, 055101 (2002).
- [10] A. Vázquez, A. Flammini, A. Maritan, and A. Vespignani, *Complexus* **1**, 38 (2003).
- [11] R. Pastor-Satorras, E. Smith, and R. V. Solé, *J. Theor. Biol.* **222**, 199 (2003).
- [12] I. Ispolatov, P. L. Krapivsky, and A. Yuryev, *Phys. Rev. E* **71**, 061911 (2005).
- [13] I. Ispolatov, P. Krapivsky, I. Mazo, and A. Yuryev, *New J. Phys.* **7**, 145 (2005).
- [14] P. L. Krapivsky and S. Redner, *Phys. Rev. E* **71**, 036118 (2005).
- [15] N. Farid and K. Christensen, *New J. Phys.* **8**, 212 (2006).
- [16] S. Cai, Z. Liu, and H. Lee, *Chaos* **25**, 083106 (2015).
- [17] U. Bhat, P. L. Krapivsky, R. Lambiotte, and S. Redner, *Phys. Rev. E* **94**, 062302 (2016).
- [18] R. V. Solé and S. Valverde, *Phil. Tran. R. Soc. B* **375**, 20190325 (2020).
- [19] D. Borrelli, *Phys. Rev. E* **111**, L032301 (2025).
- [20] D. Borrelli, eprint, arXiv:2506.15640 (2025).
- [21] E. C. de Amorim Filho, R. A. Moreira, and F. A. Santos, *J. Phys. Complex.* **3**, 025003 (2022).
- [22] F. Radicchi and S. Fortunato, *Phys. Rev. Lett.* **103**, 168701 (2009).
- [23] F. Radicchi and S. Fortunato, *Phys. Rev. E* **81**, 036110 (2010).
- [24] A. Piscitelli, A. Coniglio, A. Fierro, and M. P. Ciamarra, *Physica A* **569**, 125796 (2021).
- [25] R. A. da Costa, S. N. Dorogovtsev, A. V. Goltsev, and J. F. F. Mendes, *Phys. Rev. Lett.* **105**, 255701 (2010).
- [26] H. K. Lee, B. J. Kim, and H. Park, *Phys. Rev. E* **84**, 020101 (2011).
- [27] M. E. Newman and G. T. Barkema, *Monte Carlo methods in statistical physics* (1999).

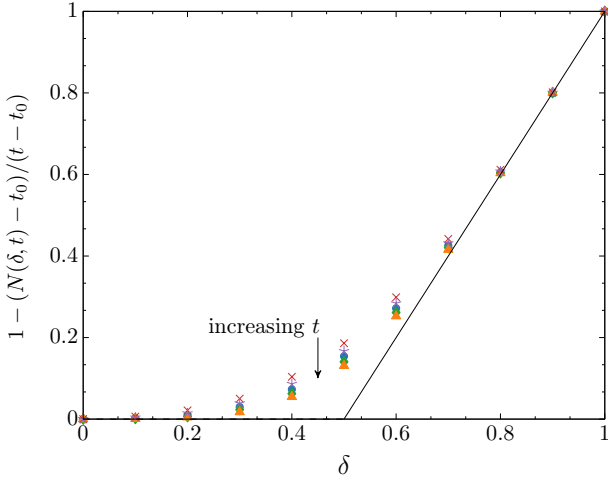


FIG. 8. Expected proportion of non-interacting vertices versus δ for various t : 256 (\times), 512 (\star), 1024 (\circ), 2048 (\diamond), 4096 (\triangle). Each point is an average over $3 \cdot 10^3$ simulations. The arrow highlights that, with increasing total number of vertices t , points from simulations would approach the theoretical behavior: solid line is obtained through $N(\delta, t)$ of Eq. (A8), whose slope was suggested in Ref. [19]; when $\delta \rightarrow 0$, simulations follow the behavior that results from Eq. (A9).

Appendix A: Continuum approach, $N(\delta, t)$

Here it is shown that (4) can be obtained through a continuum approximation, comparing it with simulations. Let $C_s(\delta, t)$ be the expected number of connected components of size s when the growing graph with divergence rate δ has a total number t of vertices.

Let $N(\delta, t)$ indicates the expected number of interacting vertices. This quantity is equivalent to the number of k -degree vertices with $k \geq 1$, which can be written as

$$N(\delta, t) = \int_{s>1} C_s(\delta, t) ds. \quad (\text{A1})$$

The total number of vertices t is instead

$$t = \int_{s>1} C_s(\delta, t) ds + C_1(\delta, t) = \int_{s \geq 1} C_s(\delta, t) ds, \quad (\text{A2})$$

where $C_1(\delta, t)$ is the number of non-interacting vertices, i.e., vertices with no edges. Then, the expected number of interacting vertices $N(\delta, t)$ also results from the total number of vertices t by subtracting $C_1(\delta, t)$, i.e.

$$N(\delta, t) = t - C_1(\delta, t). \quad (\text{A3})$$

Now, let $N_k(\delta, t)$ be the expected number of vertices with degree k when the growing graph – with divergence rate δ and divergence asymmetry rate σ – has a total number t of vertices, and let one denotes with n_k the expected fraction of vertices with degree k . Then, the rate at which the number of interacting vertices increases with t can be written as

$$\frac{\partial N(\delta, t)}{\partial t} = \int_{k \geq 1} n_k [1 - (\sigma\delta)^k - (\delta - \sigma\delta)^k] dk. \quad (\text{A4})$$

If one assumes an expected fraction of k -degree vertices $n_k \sim k^{-\gamma}$, the rate at which $N(\delta, t)$ increases with t can be written as

$$\frac{\partial N(\delta, t)}{\partial t} = \mathcal{C} \int_{k \geq 1} k^{-\gamma} [1 - (\sigma\delta)^k - (\delta - \sigma\delta)^k] dk, \quad (\text{A5})$$

with \mathcal{C} a proportionality factor; (A5) can be conveniently rewritten as

$$\begin{aligned} \frac{\partial N(\delta, t)}{\partial t} &= \mathcal{C}(1 - \delta) + \\ &+ \mathcal{C} \int_{k > 1} k^{-\gamma} [1 - (\sigma\delta)^k - (\delta - \sigma\delta)^k] dk. \end{aligned} \quad (\text{A6})$$

In the large k limit, with a prefactor 2 (from [12, 19])

$$\frac{\partial N(\delta, t)}{\partial t} \simeq 2(1 - \delta), \quad (\text{A7})$$

which yields (with $\delta \neq 1$)

$$N(\delta, t) \simeq 2(1 - \delta)t. \quad (\text{A8})$$

When instead one considers $\delta \rightarrow 0$, thus $C_1(\delta \rightarrow 0, t) \rightarrow 0$ due to a slow divergence rate which reduces the probability of generating a non-interacting vertex through duplication-divergence, then

$$N(\delta \rightarrow 0, t) = t, \quad (\text{A9})$$

which follows directly from (A3). This theoretical result is compared with numerical simulations in Fig. 8 for finite-sized graphs; for increasing size t , simulations show a behavior that approaches the theoretical prediction of (A8) and (A9). What shown here indeed was a continuum approximation that holds for increasing large values of the total number of vertices t (that includes both interacting vertices and non-interacting vertices).

Appendix B: $E(\delta, t)$, and Euler Characteristic

As in Ref. [21], Euler entropy of graphs considered here is the logarithm of the absolute value of the Euler characteristic $t - E(\delta, t)$. Eq. 5 provides an analytic form for the expected number of edges $E(\delta, t)$. Singularities in Euler entropy correspond to zeros of the Euler characteristic, occurring for $t = E(\delta, t)$. The recurrence equation for $E(\delta, t)$ can be rewritten as

$$E(\delta, t + 1) = E(\delta, t) \left(\frac{2 - 2\delta + t}{t} \right). \quad (\text{B1})$$

Starting from $t_0 = 2$, one can begin to explicit the first few iterations, beginning with $E(\delta, t_0 = 2) = 1$, and then

$$E(\delta, 3) = \left(\frac{2-2\delta+2}{2} \right), \quad (B2)$$

$$E(\delta, 4) = E(\delta, 3) \left(\frac{2-2\delta+3}{3} \right) = \left(\frac{2-2\delta+2}{2} \right) \cdot \left(\frac{2-2\delta+3}{3} \right).$$

Following the same pattern, one can continue writing Eqs. (B2) until a generic iteration t , yielding

$$E(\delta, t) = \left(\frac{2-2\delta+2}{2} \right) \cdot \left(\frac{2-2\delta+3}{3} \right) \cdot \left(\frac{2-2\delta+4}{4} \right) \cdots \left(\frac{2-2\delta+t-1}{t-1} \right), \quad (B3)$$

which can be recast as

$$E(\delta, t) = \frac{(2-2\delta+t-1) \cdot (2-2\delta+t-2) \cdots (2-2\delta+2)}{(t-1) \cdot (t-2) \cdots 2 \cdot 1}. \quad (B4)$$

By using factorial notation, it follows

$$E(\delta, t) = \frac{(1-2\delta+t)!}{(t-1)!(3-2\delta)!}. \quad (B5)$$

The factorial form of the Euler's Gamma function $\Gamma(x) = (x-1)!$ is leveraged to recast (B5), yielding

$$E(\delta, t) = \frac{\Gamma(2-2\delta+t)}{\Gamma(t)\Gamma(4-2\delta)}. \quad (B6)$$

Then, one can consider the series expansion at $t \rightarrow \infty$ of Eq. B6, which gives

$$E(\delta, t) = \frac{t^{2(1-\delta)}}{\Gamma(4-2\delta)} + \frac{t^{1-2\delta}(2\delta^2-3\delta+1)}{\Gamma(4-2\delta)} + \dots \quad (B7)$$

Considering (B7) with the first two terms of the series, for $t - E(\delta, t) = 0$ one finds a $\delta_{c,\xi} \approx 0.4421094\dots$, with $t = 1024$.

Appendix C: Second and third largest connected component

Analogous to the scaling argument for the largest connected component, one can write a scaling ansatz for the second largest connected component, the third largest connected component.

One can define the mean relative size of the second largest connected component as $P_\infty^{(2)} := N_\infty^{(2)}(\delta, t)/t$, i.e., the ratio between the mean number of vertices in the second largest connected component $N_\infty^{(2)}(\delta, t)$ and the total number of vertices t of a growing graph by duplication-divergence (symmetric coupled, $\sigma = 1/2$) with divergence probability δ . Similarly, for the third largest connected component, $P_\infty^{(3)} := N_\infty^{(3)}(\delta, t)/t$, where $N_\infty^{(3)}(\delta, t)$ is the mean number of vertices in the third largest connected component when the growing graph has total number t of vertices and divergence probability δ . With the same

critical exponents ζ, ν found for P_∞ , here the following scaling ansatz is written

$$P_\infty^{(n)}(\delta, t) = t^{\zeta/\nu} f^{(n)} \left[(\delta - \delta_c) t^{1/\nu} \right], \quad (C1)$$

where here $n = 2, 3$, and $f^{(1)}(\cdot), f^{(2)}(\cdot)$ are respectively the scaling functions for the relative size of second and third largest connected component on which one expects scaling collapse of different curves $P_\infty^{(n)}(\delta, t)$ for various size t , provided the proper choice of exponents ν, ζ and the critical value δ_c .

Recalling the exponents found for $P_\infty := P(\delta, t)$ (the largest connected component): $\nu = 9.634 \pm 0.069$, $\zeta = -0.033 \pm 0.0059$, $\delta_c = 0.6 \pm 0.002$. With this choice of ν, ζ, δ_c , Fig. 9 shows scaling collapse when plotting $P_\infty^{(n)}(\delta, t)$ versus $(\delta - \delta_c) t^{1/\nu}$; with $n = 2$ (second largest connected component), scaling collapse is on the scaling function $f^{(2)}(\cdot)$ in Fig. 9(a). With $n = 3$ (third largest connected component), scaling collapse is on the scaling function $f^{(3)}(\cdot)$ in Fig. 9(b). Remarking that $p = 1 - \delta$ would map to a bond percolation on growing graphs for which standard notation of exponents would be $\beta := \zeta$ in Eq. (8), $\gamma := \psi$ in Eq. (10), with proper adjustments.

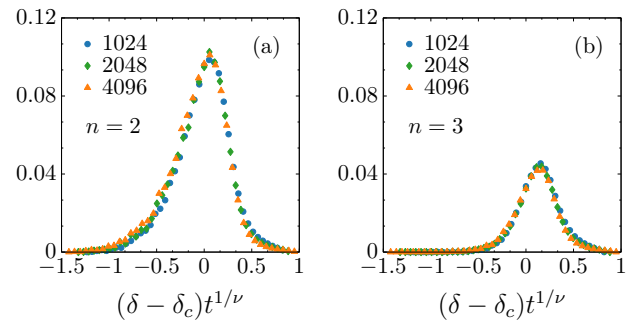


FIG. 9. Finite-size scaling for the relative size of the second largest component (a), and the third largest connected component (b); the y-axes plot $P_\infty^{(n)} t^{-\zeta/\nu}$. Points are obtained through averaging over $3 \cdot 10^3$ simulations.